Case Studies in Thermal Engineering 27 (2021) 101269

Contents lists available at ScienceDirect

Case Studies in Thermal Engineering

journal homepage: www.elsevier.com/locate/csite

Effect of pin fin configuration on thermal performance of plate pin fin heat sinks

Kitti Nilpueng [a], Mehrdad Mesgarpour [b], Lazarus Godson Asirvatham [c], Ahmet Selim Dalkılıç [d], Ho Seon Ahn [e], Omid Mahian [f,g], Somchai Wongwises [b,h,*]

[a] Department of Power Engineering Technology, King Mongkut's University of Technology North Bangkok, Bangsue, Bangkok 10800, Thailand
[b] Department of Mechanical Engineering, Faculty of Engineering, King Mongkut's University of Technology Thonburi (KMUTT), Bangmod, Bangkok 10140, Thailand
[c] Department of Mechanical Engineering, Karunya Institute of Technology and Sciences, Coimbatore, Tamil Nadu, India
[d] Department of Mechanical Engineering, Yildiz Technical University, Yildiz, Besiktas, Istanbul, Turkey
[e] Department of Mechanical Engineering, Incheon National University, Incheon, Republic of Korea
[f] School of Chemical Engineering and Technology, Xi'an Jiaotong University, Xi'an, China
[g] Department of Mechanical Engineering, Center for Nanotechnology in Renewable Energies, Ferdowsi University of Mashhad, Mashhad, Iran
[h] National Science and Technology Development Agency (NSTDA), Pathum Thani 12120, Thailand

GRAPHICAL ABSTRACT

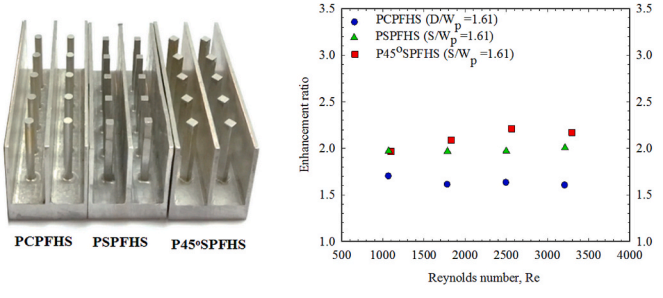

ARTICLE INFO

Keywords:
Flow visualization
Heat transfer enhancement
Heat transfer coefficient
Thermal performance

ABSTRACT

Flow behavior and heat transfer characteristics of air flow inside the plate pin fin heat sinks (PPFHS) are presented. The effects of pin fin shape, pin fin orientation, and ratio of distance between pin and plate fin center to pin fin size (S/D_p or S/W_p) on the flow pattern, heat transfer coefficient (HTC), pressure drop (ΔP) and thermal performance are investigated. Three types of

* Corresponding author. Department of Mechanical Engineering, Faculty of Engineering, King Mongkut's University of Technology Thonburi (KMUTT), Bangmod, Bangkok, 10140, Thailand. Tel.: +6624709115.
E-mail address: Somchai.won@kmutt.ac.th (S. Wongwises).

https://doi.org/10.1016/j.csite.2021.101269
Received 2 August 2020; Received in revised form 30 May 2021; Accepted 18 July 2021
Available online 19 July 2021

pin fin shape, including a circular pin, square pin, and 45° square pin with pin fin sizes of 2.5, 3.0, and 3.5 mm, are used. The flow visualization used smoke to study the air flow behavior inside the PPFHS. The test runs were done at a heat flux of 14.81 kW/m^2 and Reynolds number (Re) ranging between 1700 and 5200. Under the same pin fin frontal area, the HTC and ΔP of air inside the plate square pin fin heat sink (PSPFHS) was higher than that from the plate circular pin fin heat sink (PCPFHS) by an average of 12.52 and 15.05%, respectively. The decrease of the S/D_p or S/W_p from 2.25 to 1.61 caused the augmentation of the HTC and ΔP of air flow inside the PPFHS by about 11.77%–17.17% and 46.61%–50.52%, respectively. The average thermal performance factors (TPF) were 1.32, 1.44, and 1.42 for PCPFHS, PSPFHS, and the plate 45° square pin fin heat sink (P45°SPFHS), respectively. The correlations for Nusselt number (*Nu*) and friction factor (*f*) were also proposed.

Nomenclature

A_{HS}	Heat transfer surface area of heat sink, [m^2]
$c_{p,a}$	Specific heat of air, [J/kg K]
D_p	Pin fin diameter, [m]
D_H	Hydraulic diameter, [m]
f	Friction factor
f_0	Friction factor of PFHS
k	Thermal conductivity, [W/m K]
h	Heat transfer coefficient, [W/m^{2}K]
H_b	Heat sink base height, [m]
H_f	Fin height, [m]
L	Length of heat sink, [m]
PCPFHS	Plate circular pin fin heat sink
PSPFHS	Plate square pin fin heat sink
P45°SPFHS	Plate 45° square pin fin heat sink
ΔP	Pressure drop, [Pa]
p_c	Flow channel perimeter, [m]
p_p	Pin pitch, [m]
Q	Peat transfer rate, [W]
$\dot{m}_a$	Mass flow rate of air, [kg/s]
Re	Reynolds number
$T_{a,mean}$	Average temperature of air inside the channel, [K]
$T_{ai,mean}$	Average temperature of air at inlet, [K]
$T_{ao,mean}$	Average temperature of air at outlet, [K]
$T_{b,mean}$	Average temperature of heat sink base surface, [K]
Nu	Nusselt number of PPFHS
Nu_0	Nusselt number of PFHS
t_f	Fin thickness, m
TPF	Thermal performance factor
V	Velocity of air, [m/s]
W_p	Pin fin width, [m]

1. Introduction

Heat sink is a type of heat exchanger that is designed and used as a cooling system in electronic devices, such as central processing units (CPU), electronic chips, and power transistors. Normally, plate fin heat sinks (PFHS) with air force convections are widely used in industrial applications. This is because of its simplicity compared with liquid cooling systems and heat pipes [1,2]. With the continuous growth of modern electronic technology, small and high performance electronic devices have been developed by many manufacturers. Under high heat generation and the limitations of the heat transfer area, the working temperature may exceed the limits and cause some mechanism failures in electronic devices. To obtain reliable operations and a long lifetime of modern electronic components, the appropriate design of air cooling system is very important. In the past, many research works have considered the influence of geometry parameters on the optimum conditions of PFHS. For instance, Li and Chao [3] presented the performance of PFHS of cooling air in a cross flow. The influences of the Re, the width and height of fin on the ΔP and the thermal resistance were reported. The results found that the thermal performance (TP) was augmented when increasing the Re. But, the enhancement of TP was limited when the Re

reached a certain valve. The higher fins gave a higher TP under the constant fin width. The effect of varying the fin thickness along the fin height on optimum TP of a PFHS was studied numerically by Kim et al. [4]. The results revealed the thermal resistance was decreased by approximately 15%, compared with the constant fin thickness. The thermal resistances also decreased when increasing the frontal area aspect ratio.

In order to get better heat sink thermal performance, heat transfer enhancement techniques have been applied to a PFHS by some researchers. Yang et al. [5] presented the heat transfer performance of PFHS at different fin types. They stated that the performance of the plain fin was greater than the interrupted fin and dense vortex generator. The optimum design enhancement was the triangular attack vortex generator. The heat transfer of a PFHS with vortex generators (VG) was studied by Li et al. [6]. The heat transfer rate was enhanced by using VG; however, the increase of the ΔP was slight at low Re. They stated the optimum working conditions obtained a 30° attack angle of VG. Nilpueng and Wongwises [7] examined the influence of twist ratio and perforation diameter on the optimum TP of a PFHS with twisted tape. The enhancement ratio increased with decreasing twist ratio under the same perforation diameter. Chingulpitak et al. [8] presented the heat transfers and flow mechanisms of air flow through crosscut heat sinks. The effects of crosscut length, crosscuts number, and the Re on thermal resistance and pressure were studied. The flow visualization of air inside the crosscut heat sink was also presented. They stated that the optimum ratio of thermal resistance appeared when the crosscut length ranged between 1.5 mm and 2.0 mm. Ahmed [9] numerically investigated the performance of the PFHS inserted with ribs. The influences of numbers, sizes, orientations, and positions of the ribs on the TP were presented. The TP of the ribbed PFHS was about 1.55 times higher than the PFHS. However, the TP enhancement was decreased when increasing the ribs number. Yu et al. [10] presented the analytic solutions of the *Nu* and *f* of the fluid flow inside a wavy plate fin. The Poiseuille number (Po) and *Nu* were validated with numerical simulations. The influence of the ratio of fin spacing to period length on the Po, *Nu*, and streamlines and velocity profiles was studied. The *Nu* was increased to a maximum value before decreasing when the ratio of fin spacing to the period length increased. Keawkamrop et al. [11] studied the TP of crimped spiral fin and tube heat exchangers. The fin pitches were varied between 3.18 and 6.35 mm. The correlation of Nu and Colburn factor were proposed. Yang and Peng [2] presented the enhancement of heat transfer of the PCPFHS. The synthetic performance of the PCPFHS was greater than that of the PFHS. Also, the performance of the in-line arrangement was greater than the staggered arrangement. The comparison of TP between the PPFHS and PFHS was simulated by Yu et al. [12]. The circular pin fin configuration was used. The thermal resistance of PPFHS was lower than that obtained from the PFHS by approximately 30%. They concluded that to obtain better air-cooling results, unsuitable PFHS were easy to replace by the PPFHS. Zhou et al. [13] numerically investigated the TP of PPFHS. Five patterns of pin configurations, including circular, square, NACA 0050, elliptic, and dropform, were used. The *Nu* of the PPFHS was higher than that of the PFHS by about 35% under the same Re. Yuan et al. [14] studied the performance of a PCPFHS. The potential of PPFHS was assessed by FLUENT. The testing conditions were performed at a temperature less than 358 K and a velocity higher than 6.5 m/s. The pin height had a major impact on the TP of heat sink. The effect of pin fin interruptions on the TP of straight and wavy miniature heat sinks was presented by Khoshvaght-Aliabadi et al. [15]. Three different interruptions were performed at Re ranging between 100 and 900. The results of heat transfer parameters were presented and compared. They reported that the TP of the PFHS with pin fin interruption was greater than that obtained from the original PFHS.

As previously discussed above, although several enhancement techniques have been applied to improve the PFHS thermal performance, they might not work properly at high heat flux. Consequently, the PPFHS which has been a new type of heat sink, has been designed and developed for working under this condition. It is very attractive because the thermal resistance of PPFHS is lower than the PFHS by about 30% [12]. However, to obtain optimum PPFHS thermal performance, the information of the proper pin fin configurations and working conditions are still needed. Although some information concerning the PPFHS thermal performance is currently available, there remains room for further research, especially the flow visualization and the relationship between the flow pattern and heat transfer mechanism inside the PPFHS remains unstudied. Moreover, some aspects relating to the concerned studies are still lacking e.g. the effect of the ratio of the distance between pin and plate fin center (S) to pin fin size (D_p or W_p). In the present study,

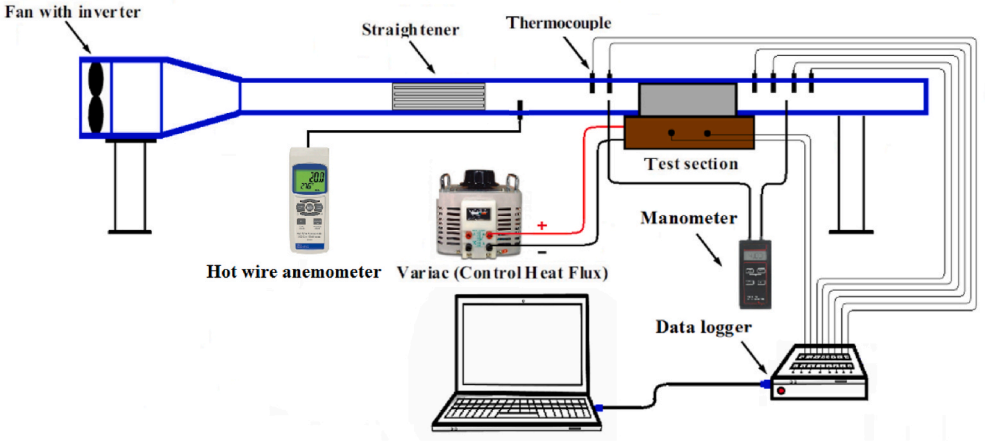

Fig. 1. Schematic diagram of experimental apparatus. [From Nilpueng et al. [16], with permission from Elsevier].

main aim is to investigate the heat transfer and flow mechanism of air flow inside PPFHS. Three different pin fin shapes, including circular pin, square pin, and 45° square pin, are experimentally studied. Flow visualization using smoke was performed to observe the flow mechanism of air flow inside the PPFHS. The effect of air velocity, pin fin shape, pin fin orientation, and ratio of distance between pin and plate fin center to pin fin size on the ΔP, HTC, and thermal performance were investigated. The correlations for predicting the *Nu* and *f* for PCPFHS, PSPFHS P45°SPFHS were also proposed.

2. Experimental apparatus

To investigate the effect of pin fin configuration on the performance of PPFHS, the experimental apparatus as reported in Nilpueng et al. [16] is used in the experiment (Fig. 1). It consists of two main parts: wind tunnels and heat sinks.

2.1. Wind tunnel

The open type rectangular wind tunnel is constructed with an acrylic plate. The flow area and length of the rectangular channel are 675 mm^2 and 0.8 m. The wind tunnel is enclosed with insulation to minimize heat loss. A fan was connected with an inverter to regulate the velocity at the entrance. The air velocity ranged from 1 to 6 m/s. A straightener was used to straighten the air flow and obtain a uniform flow. The air velocity was measured by a hot wire anemometer with an accuracy of ±1.0%. A digital manometer with an accuracy of ±0.5% was used to measure the pressure drop across the heat sinks. Six T-type thermocouples with an uncertainty of ±0.1 °C were installed to measure the mean air temperature at the entrance and exit. Two thermocouples are equipped at the center core of flow channel and a distance of 20 and 40 mm before entering the test section. Similarly, four thermocouples are equipped at a distance of 20, 40, 60 and 80 mm after leaving the test section, respectively.

2.2. Heat sinks

In this experiment, two main types of heat sinks, PFHS and PPFHS, were used (Fig. 2a and b). For PPFHS, three different pin fin shapes, including circular pin, square pin, and 45° square pin, were experimentally studied (Fig. 2c). Ten aluminum heat sinks were fabricated by using a CNC milling machine. Details of the heat sink dimensions, including length (*L*), width (*W*), base height (H_b), fin

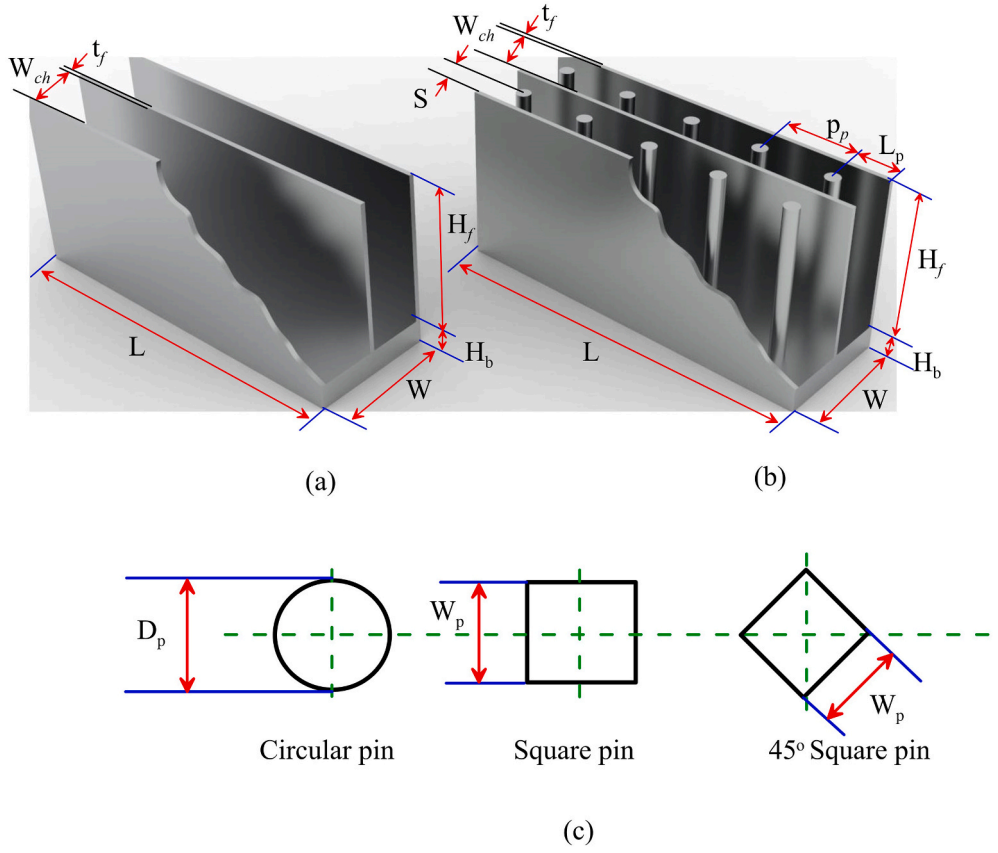

Fig. 2. Two types of heat sinks.

height (H_f), fin thickness (t_f), channel width between plate fins (W_{ch}), pin pitch (p_p), pin size (pin fin diameter, D_p or pin fin width, W_p) and the distance between pin and plate fin center (S) of a PFHS, three plate circular pin fin heat sinks (PCPFHS), three plate square pin fin heat sinks (PSPFHS), and three plate 45° square pin fin heat sinks (P45°SPFHS), are shown in Table .1. To study the effect of pin fin dimension, the circular pin diameters (D_p) of 2.5, 3, and 3.5 mm and the square pin width (W_p) of 2.5, 3, and 3.5 mm were made. A 100 W plate heater was attached at the base surface and covered with insulation. Thermal grease paste compound silicon was used to increase the conduction heat transfer between the surface of the plate heater and the base surface of the heat sink. The electric power was measured by a power meter with an accuracy of ±0.08 kW. The supplied heat flux to the heat sink was the plate heater's electric power per the heat transfer surface area. The supplied heat flux was controlled at 14.81 kW/m^2 by using a variable AC transformer. Four T-type thermocouples with an uncertainty of ±0.1 °C were mounted at a 4.5 mm height from the bottom of the heat sink base. All data were collected at a steady state.

3. Data reduction

The HTC obtained from the heat sinks is determined by

$$h = \frac{Q}{\eta_o A_{HS}\left(T_{b,mean} - T_{a,mean}\right)} \tag{1}$$

$$T_{a,mean} = \left(T_{ai,mean} + T_{ao,mean}\right)/2 \tag{2}$$

where $T_{a,mean}$ is the mean temperature of air inside the channel, A_{HS} is the heat transfer surface area, $T_{b,mean}$ is the mean temperature of the heat sink base surface and η_o is the surface efficiency which is assumed as 100% when the thermal conductivity (k) is high, the fin length (L) is low and the ratio of fin area to total area (A_f/A_t) is not high. The heat transfer rate (Q) is the multiplication of mass flow rate ($\dot{m}_a$), specific heat ($c_{p,a}$) and temperature difference of air at the outlet and inlet ($T_{ao,mean}$ - $T_{ai,mean}$) as followed:

$$Q = \dot{m}_a c_{p,a}\left(T_{ao,mean} - T_{ai,mean}\right) \tag{3}$$

Based on the energy balance, the difference between the heat transfer rate provided by heater and the heat transfer rate received by air flow is the heat loss. The heat loss of the heat sink to the surrounding is about 3%–7%.

The Nusselt number can be calculated from:

$$Nu = \frac{hD_H}{k} \tag{4}$$

$$D_H = \frac{4A_c}{p_c} \tag{5}$$

where k is the thermal conductivity, D_H is the hydraulic diameter of the flow channel, A_c is the minimum free flow area, and p_c is the perimeter of the minimum free flow channel.

The friction factor is calculated by the followed equation:

$$f = \frac{\Delta P}{4\left(\frac{L}{D_H}\rho\frac{V^2}{2}\right)} \tag{6}$$

$$\mathrm{Re} = \frac{\rho V D_H}{\mu} \tag{7}$$

where ΔP is the pressure drop, V is the average frontal velocity of the air between the fins, ρ is air density, L is the heat sink length, and μ is air viscosity.

Table 1
Dimensions of test sections (mm).

Test sections	L	W	H_b	H_f	W_{ch}	t_f	L_p	p_p	S	D_p	W_p	D_H
1. PFHS	75	27	7.5	25	11.25	1.5	–	–	–	–	–	15.5
2. PCPFHS	75	27	7.5	25	11.25	1.5	12.5	12.5	5.63	2.5	–	7.45
3. PCPFHS	75	27	7.5	25	11.25	1.5	12.5	12.5	5.63	3.0	–	7.08
4. PCPFHS	75	27	7.5	25	11.25	1.5	12.5	12.5	5.63	3.5	–	6.71
5. PSPFHS	75	27	7.5	25	11.25	1.5	12.5	12.5	5.63	–	2.5	7.45
6. PSPFHS	75	27	7.5	25	11.25	1.5	12.5	12.5	5.63	–	3.0	7.08
7. PSPFHS	75	27	7.5	25	11.25	1.5	12.5	12.5	5.63	–	3.5	6.71
8. P45°SPFHS	75	27	7.5	25	11.25	1.5	12.5	12.5	5.63	–	2.5	6.68
9. P45°SPFHS	75	27	7.5	25	11.25	1.5	12.5	12.5	5.63	–	3.0	6.15
10.P45°SPFHS	75	27	7.5	25	11.25	1.5	12.5	12.5	5.63	–	3.5	5.60

The thermal performance was evaluated in term of dimensionless thermal performance factor (TPF) as

$$TPF = \frac{(Nu/Nu_0)}{(f/f_0)^{1/3}} \tag{8}$$

where Nu and f are the Nusselt number and the friction factor of PPFHS. Nu_0 and f_0 are the Nusselt number and the friction factor of PFHS. The uncertainties of the experimental data were calculated by the root mean sum square method. The mean relative uncertainties of the HTC and ΔP are ±6.42%, and ±0.5%, respectively.

4. Results and discussion

4.1. Flow pattern

To observe the air flow pattern inside the PPFHS, the flow visualizations using smoke were used, and the details of the flow behavior were registered by a video camera and digital camera. The air flow behavior inside the flow channel of PPFHS was divided into two segments. That is, air flows between the pin and plate fin and the flow of air past the pin fin. It was found that the flow of air split into two streams and attached to the pin fin body shape as air impinged the front of the first pin fin (Fig. 3). After that, the air separated from the pin fin body (separation flow), which resulted in a recirculation flow and backflow (a wake region) in the rear

(a) Plate circular pin fin heat sink (PCPFHS) **with D_p = 3.5 mm**

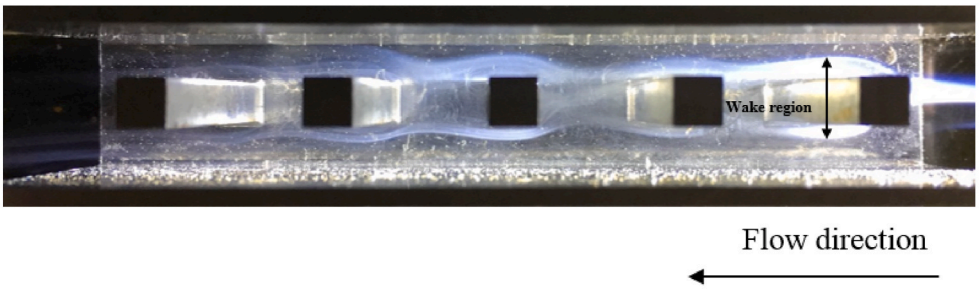

(b) Plate square pin fin heat sink **(PSPFHS) with W_p = 3.5 mm**

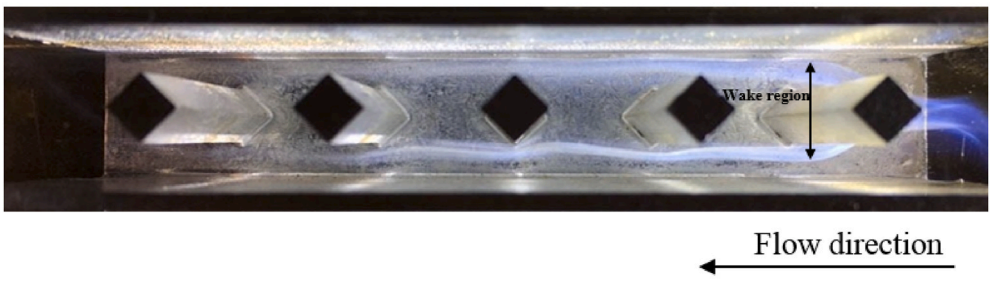

(c) Plate 45° square pin fin heat sink **(P45°SPFHS) with W_p = 3. 5 mm**

Fig. 3. Flow patterns of air inside the plate pin fin heat sink (PPFHS) at air velocity of 0.5 m/s.

portion of the pin fin. Two streams of air tended to converge before it impinged the next pin fins. It is observed from the video footage that the impingement flow of two streams of air at the pin fin region led to the disturbance and mixing of the air flow between the plate and pin fins. Considering the effect of the pin fin shape under the same pin fin frontal area showed that the disturbance of air flow between the pin fin and plate fin and the occurrence of a wake region behind the square pin fin was greater than that from the circular pin fin (Fig. 3a and b). The rotation of the square pin (P45°PFHS) led to a larger wake region and a narrower flow channel between the plate and pin fins compared to the square pin fin (Fig. 3b and c). This resulted in the higher air velocity and stronger interaction of the impingement flow at the pin fin and air flow between the plate and pin fins. Also, the turbulence of air flow along the gap between the plate and pin fins and wake region behind the pin fin was larger when decreasing the ratio of S/D_p (Fig. 4).

4.2. Heat transfer and flow characteristics

The experimental data of the HTC and ΔP of the PFHS were compared with the correlations from Teertstra et al. [17] and Wu et al. [18]. The tendency of measured data and previous correlations were consistence with a mean absolute deviation (MAD) of 7.77 and 10.15% for the HTC and ΔP, respectively. The comparison between the experimental data and previous correlations indicated that the experimental apparatus was reasonably accurate.

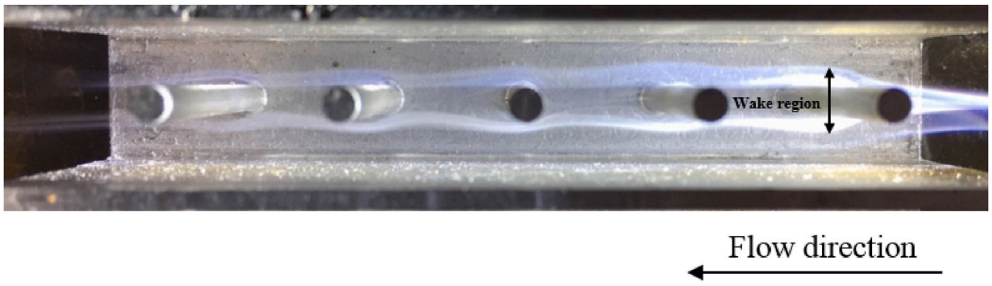

(a) Plate circular pin fin heat sink **(PCPFHS) with S/D_p = 2.25**

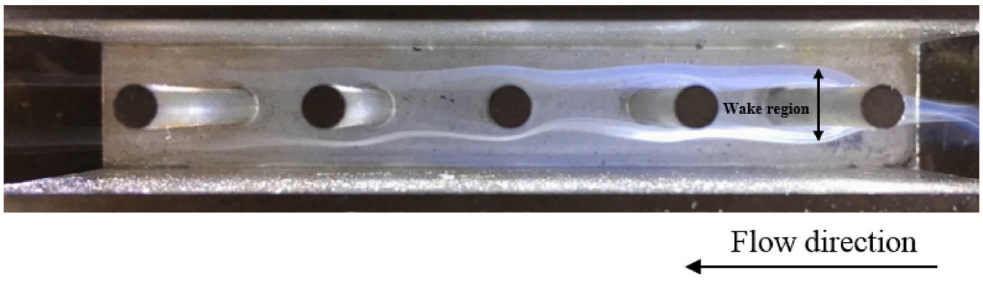

(b) Plate circular pin fin heat sink **(PCPFHS) with S/D_p = 1.78**

(c) Plate circular pin fin heat sink **(PCPFHS) with S/D_p = 1.61**

Fig. 4. Effect of S/D_p on flow behavior inside the Plate circular pin fin heat sink (PCPFHS) at air velocity of 0.5 m/s.

4.2.1. Influence of pin fin shape

The HTC and ΔP obtained from the PCPFHS and PSPFHS were compared, as shown in Fig. 5. The HTC and ΔP were found to increase when the air velocity varied. This was because the increase of the air velocity caused the enhancement of the turbulent intensity of the air flowing in the channel. Consequently, the HTC and ΔP were increased. Based on the comparison of the pin fin shape,

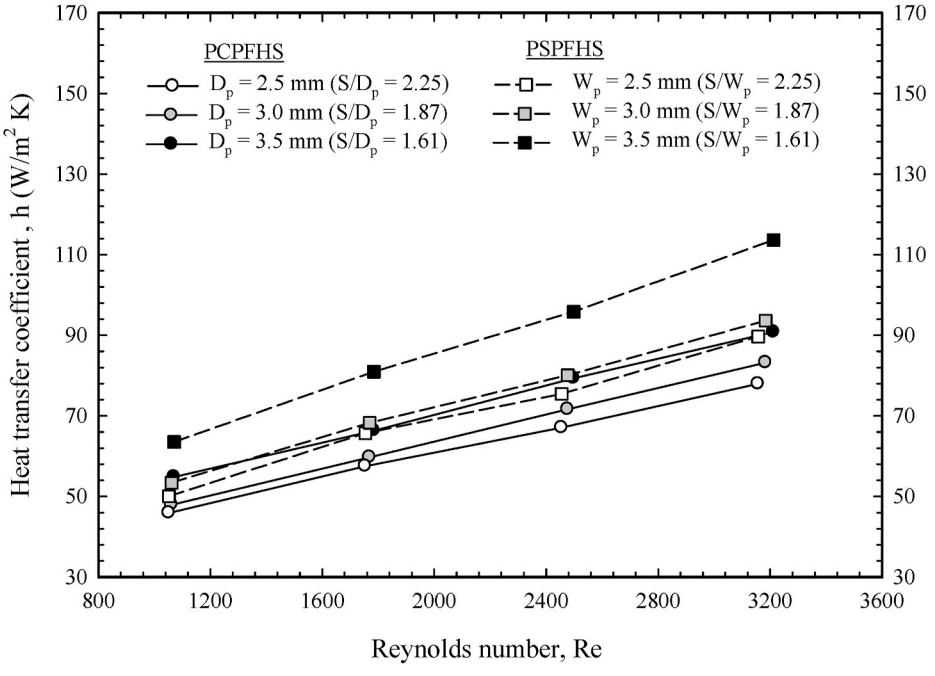

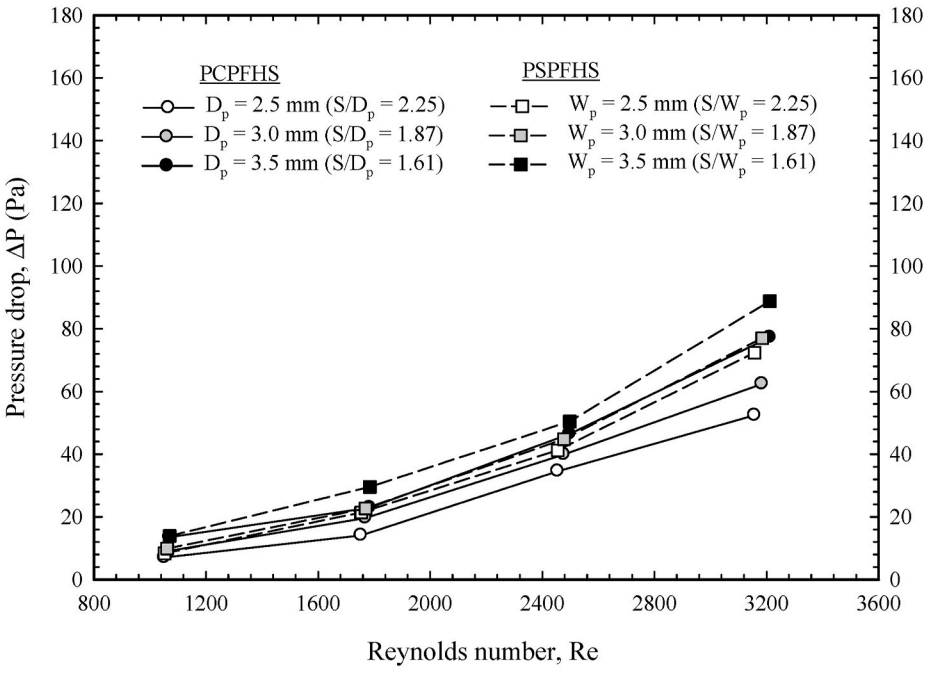

Fig. 5. Effect of pin fin configuration on HTC and ΔP.

the heat sinks had the same pin fin length, pin fin pitch, and pin fin frontal area. Under the similar Re, the HTC and the ΔP of the air inside the PSPFHS were higher than that from the PCPFHS by an average of 12.52% and 15.05%. This can be explained by the flow behavior of the air inside the PPFHS. According to the flow visualization from Fig. 3a and b, the interaction of the impingement flow at the pin fin region and the flow between the plate and pin fins obtained from the PSPFHS were higher than that from the PCPFHS. This

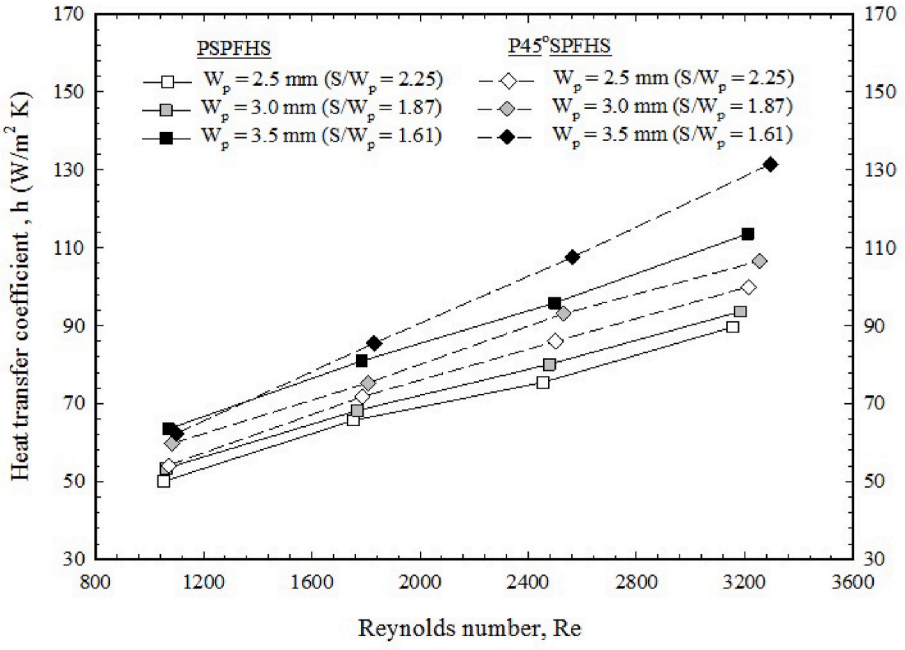

(a)

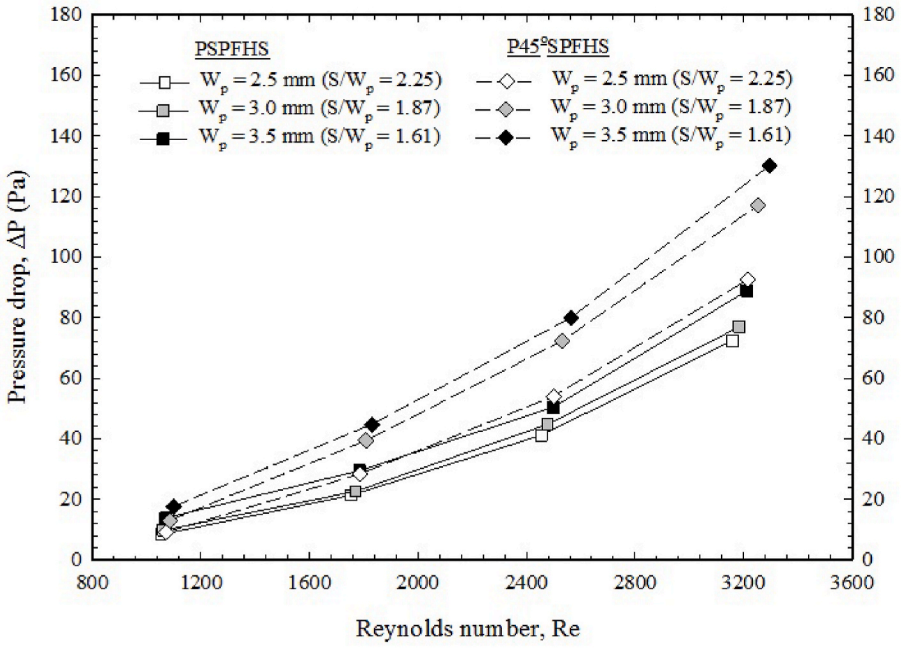

(b)

Fig. 6. Effect of pin fin orientation on HTC and ΔP.

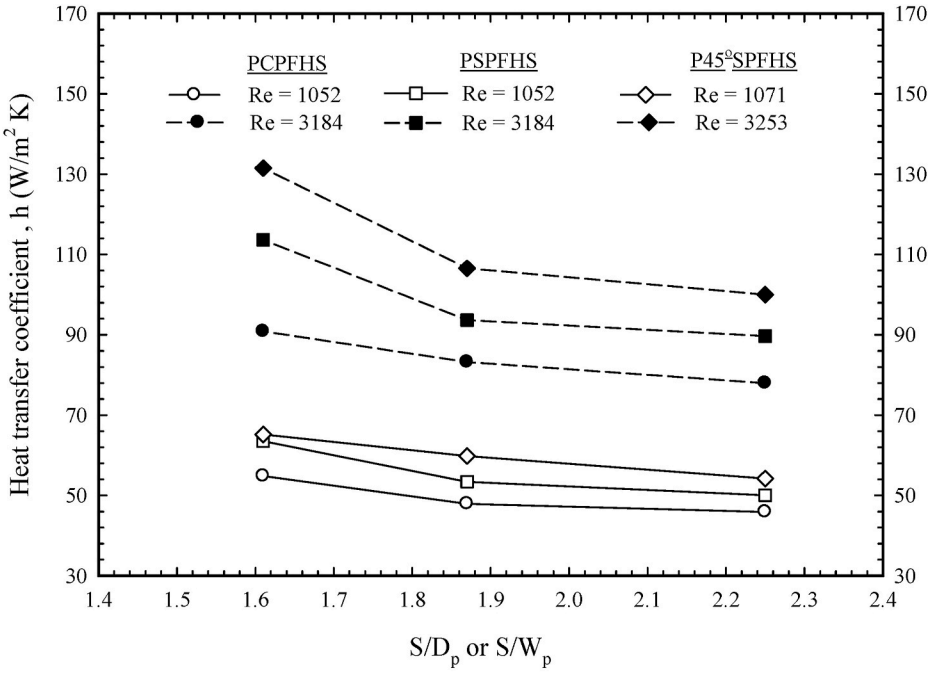

(a)

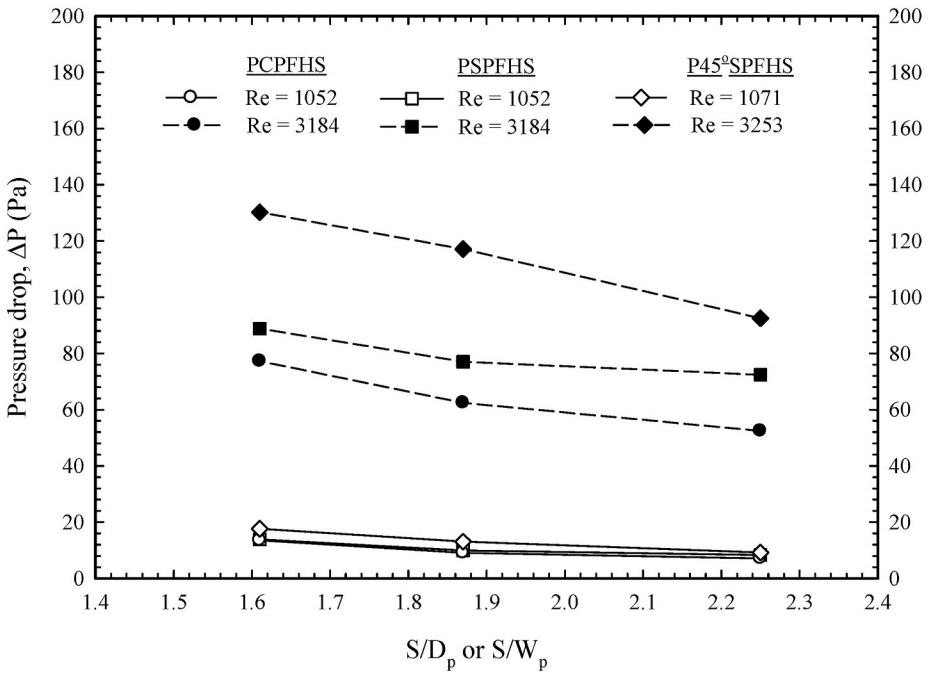

(b)

Fig. 7. Effect of S/D_p or S/W_p on HTC and Δp.

caused higher mixing of air flow between the plate and pin fins. Moreover, it was also found that the wake region behind the pin fin obtained from the PSPFHS were greater than that obtained from the PCPFHS. This resulted in the higher pressure drop due to inertial drag. Therefore, the HTC and ΔP of the PSPFHS were higher than that obtained from the PCPFHS.

4.2.2. Influence of pin fin orientation

The comparison between the plate square pin fin heat sink with 0° (PSPFHS) and plate fin heat sink with 45° square pin (P45°SPFHS) was presented under the same pin fin length, pin fin width, and pin fin pitch as shown in Fig. 6. Considering the effect of the pin fin orientation, it was clearly seen that the HTC and ΔP at a 45° angle of attack was increased by about 13.09 and 54.81% when compared to a 0° angle of attack. This was because the frontal area of the 45° square pin was higher than the square pin. Conversely, the flow channel between the plate and pin fins of P45°SPFHS were narrower than the PSPFHS. This gave rise to a higher air velocity between the plate and pin fins and a higher mixing of the impingement flow at the pin fin region and the air flow between the plate and pin fins. It is also observed from the figure that the wake region of the 45° square pin was greater than the square pin. This indicated that the pressure drop due to inertial drag was higher. These resulted in the enhancement of the HTC and ΔP inside the flow channel.

4.2.3. Influence of the ratio of S/D_p or S/W_p

Considering the effect of S/D_P or S/W_p of PCPFHS, PSPFHS, and P45°SPFHS in Fig. 7, we found that the HTC and ΔP of air inside the flow channel were enhanced when the S/D_P or S/W_p was decreased from 2.25 to 1.61. When comparing to the S/D_P or S/W_p of 2.25, the HTC increased by about 11.77, 16.21, and 17.17% for the PCPFHS, PSPFHS, and P45°SPFHS, respectively. Similarly, the pressure was increased by about 46.61, 28.40, and 50.52% for PCPFHS, PSPFHS, and P45°SPFHS, respectively. This was because the decrease of S/D_P or S/W_p resulted in a higher air velocity between the plate and pin fin and larger wake region. As a result, the flow of air between the plate and pin fin was also greatly disturbed by the impingement of airflow at pin fin region. This flow behavior led to the heat transfer enhancement inside the fin heat sink. In addition, it was found that the larger wake region in the rear portion of the pin fin resulted in the higher pressure drop due to inertial drag. These impacts caused the HTC and ΔP to increase. Moreover, it was observed that the enhancement of the HTC and ΔP also depended on the Re. This meant that the high Re also caused the high HTC and ΔP under the same S/D_P or S/W_p.

4.3. Heat sink performance

In order to compare the heat transfer rate between PPFHS and PFHS, the ratio of Nu_{PPFHS}/Nu_{PFHS} (enhancement ratio) of all heat sink at different the S/D_P or S/W_p were assessed. The experimental result showed that the enhancement ratio increased when the S/D_P or S/W_p were decreased. The *Nu* of PCPFHS, PSPFHS, and P45°SPFHS was greater than that of PFHS by an average of 49.9%, 72.8%, and 90.79%. This was due to the inserting the pin fin among the plate fin and the decrease of the S/D_P or S/W_p ratio resulted in the higher turbulence and mixing of air flow between plate and pin fin. As a result, the *Nu* of PPFHS was higher than that of PFHS.

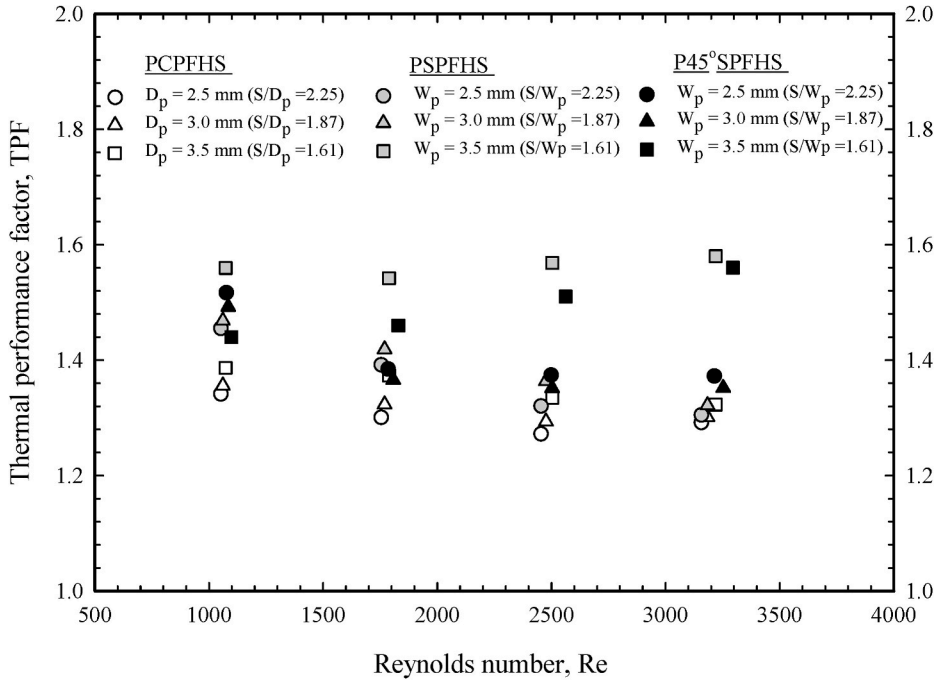

Fig. 8. Thermal performance factor versus Reynolds number.

The thermal performance factor (TPF) was used to evaluate the thermal performance of the PPFHS. The TPF was defined as the ratio of the *Nu* and *f* of the PPFHS and PFHS ($(Nu/Nu_0)/(f/f_0)^{1/3}$). It can be seen from Fig. 8 that the TPF of all PPFHS were higher than 1. This means that the thermal performance of all PPFHS were higher than PFHS. The TPF of the PPFHS tended to slightly decrease with increasing Re. However, the TPF tended to slightly increase for P45°SPFHS at a 3.5 mm pin fin size, whereas the TPF was nearly constant for PSPFHS at a 3.5 mm pin fin size. It may be concluded that the tendency of the TPF of PSPFHS and P45°SPFHS was changed when the ratio of S/W_p was 1.61. When considering the average TPF of PPFHS, it was found that the average TPF of PCPFHS, PSPFHS, and P45°SPFHS were 1.32, 1.44, and 1.42. This indicated that PSPFHS had the highest average TPF. It also implied that the thermal performance of PSPFHS was higher than PCPFHS under the same pin fin frontal area. Moreover, the thermal performance of PSPFHS with a 0° angle of attack was slightly higher than that of PSPFHS with a 45° angle of attack. In addition, when considering the TPF of each PPFHS, the optimum conditions occurred at S/D_P of 1.61 and low Re for PCPFHS, at S/W_P of 1.61 and all Re for PSPFHS, and at S/W_P of 1.61and high Re for P45°SPFHS.

4.4. Nusselt number and friction factor correlations

The correlations of *Nu* and *f* for PPFHS were developed in term of Re, Pr, and S/D_p or S/W_P as presented in Table 2. The predicted Nusselt number agreed with the measured data with mean absolute errors (MAE) of ±1.77%, ±3.13% and ±2.56% for PCPFHS, PSPFHS, and P45°SPFHS, and all data points were within the ±10% deviation. Similarly, for the friction factor, the results illustrated that 95% of the data were within a deviation of ±15%, and the MAE was ±8.51%, ±5.33% and ±7.88% for PCPFHS, PSPFHS, and P45°SPFHS, respectively.

5. Conclusions

The effects of the pin fin shape, pin fin orientation, and ratio of distance between pin and plate fin center to pin fin size (S/D_p or S/W_p) on flow behavior, HTC, and ΔP of air inside the PPFHS are presented. Three types of pin fin, including circular pin, square pin, and 45° square pin, with different pin fin sizes were used. The experiment was performed at a supplied heat flux of 14.81 kW/m^2 and a Re ranging between 1700 and 5200. The results obtained from the present study can be concluded as follows:

1) The air flow behavior inside the flow channel of PPFHS can be separated into two parts: air flow along the gap between the pin and plate fin and the flow of air past the pin fin. The interaction of air flow between the plate and pin fins and the impingement flow at the pin fin was higher when decreasing the ratio of S/D_p or S/W_p.
2) The comparison of the pin fin shape between the PCPFHS and PSPFHS found that the HTC and ΔP of air inside the PSPFHS was higher than that from the PCPFHS by an average of 12.52% and 15.05%, respectively.
3) The HTC and ΔP of PSPFHS were increased as the angle of attack increased. The HTC and ΔP of the P45°SPFHS were found to increase by about 13.09% and 54.81%, compared to PSPFHS.
4) The decrease of the S/D_P or S/W_p from 2.25 to 1.61 caused the enhancement of the HTC and ΔP of air flow inside the flow channel. When comparing to the S/D_P or S/W_p of 2.25, the HTC and ΔP were increased by about 11.77%, 16.21%, and 17.17% and 46.61%, 28.40%, and 50.52%, for the PCPFHS, PSPFHS, and P45°SPFHS, respectively.
5) The average enhancement ratio was 1.50, 1.73, and 1.91, for PCPFHS, PSPFHS, and P45°SPFHS, respectively. While, the average TPF of PCPFHS, PSPFHS, and P45°SPFHS were 1.32, 1.44, and 1.42, respectively.

Author statement

Kitti Nilpueng: Experiment, Writing – original draft. Mehrdad Mesgapour: Investigation. Lazarus Godson Asirvatham: Investigation. Ahmet Selim Dalkılıç: Investigation. Ho Seon Ahn: Investigation. Omid Mahian: Investigation. Somchai Wongwises: Investigation, Writing – review & editing.

Declaration of competing interest

The authors declare that they have no known competing financial interests or personal relationships that could have appeared to influence the work reported in this paper.

Table 2
Correlations for Nusselt number and friction factor.

Heat sink	Nusselt number	friction factor
PCPFHS	$Nu = 0.586Re^{0.478}Pr^{1/3}(S/D_p)^{-0.137}$	$f = 1.153Re^{-0.238}(S/D_p)^{-0.342}$
PSPFHS	$Nu = 0.586Re^{0.514}Pr^{1/3}(S/W_p)^{-0.339}$	$f = 0.758Re^{-0.161}(S/W_p)^{0.107}$
P45°SPFHS	$Nu = 0.262Re^{0.586}Pr^{1/3}(S/W_p)^{-0.026}$	$f = 0.187Re^{-0.012}(S/W_p)^{0.335}$

Acknowledgments

The first author thanks the College of Industrial Technology, King Mongkut's University of Technology North Bangkok, Thailand for Grant No. Res-CIT 0241/2019. The authors acknowledge the support provided by the "Research Chair Grant" National Science and Technology Development Agency (NSTDA) and the "KMUTT 55th Anniversary Commemorative Fund.

References

[1] A. Al-damook, F.S. Alkasmoul, Heat transfer and air flow characteristics enhancement of compact plate-pin fins heat sinks – a review, Propulsion and Power Research 7 (2018) 138–146.
[2] Y.T. Yang, H.S. Peng, Investigation of planted pin fins for heat transfer enhancement in plate fin heat sink, Microelectron. Reliab. 49 (2009) 163–169.
[3] H.-Y. Li, S.-M. Chao, Measurement of performance of plate-fin heat sinks with cross flow cooling, Int. J. Heat Mass Tran. 52 (2009) 2949–2955.
[4] D.-K. Kim, J. Jung, S.J. Kim, Thermal optimization of plate-fin heat sinks with variable fin thickness, Int. J. Heat Mass Tran. 53 (2010) 5988–5995.
[5] K.-S. Yang, S.-L. Li, I.Y. Chen, K.-H. Chien, R. Huc, C.-C. Wang, An experimental investigation of air cooling thermal module using various enhancements at low Reynolds number region, Int. J. Heat Mass Tran. 53 (2010) 5675–5681.
[6] H.-Y. Li, C.-L. Chen, S.-M. Chao, G.-F. Liang, Enhancing heat transfer in a plate-fin heat sink using delta winglet vortex generators, Int. J. Heat Mass Tran. 67 (2013) 666–677.
[7] K. Nilpueng, S. Wongwises, Thermal performance investigation of a plate fin heat sink equipped with twisted tape and perforated twisted tape, J. Therm. Sci. Technol. 16 (2021) 1–12.
[8] S. Chingulpitak, N. Chimres, K. Nilpueng, S. Wongwises, Experimental and numerical investigations of heat transfer and flow characteristics of cross-cut heat sinks, Int. J. Heat Mass Tran. 102 (2016) 142–153.
[9] H.E. Ahmed, Optimization of thermal design of ribbed flat-plate fin heat sink, Appl. Therm. Eng. 102 (2016) 1422–1432.
[10] D. Yu, W. Jeon, S.J. Kim, Analytic solutions of the friction factor and the Nusselt number for the low-Reynolds number flow between two wavy plate fins, Int. J. Heat Mass Tran. 115 (2017) 307–316.
[11] T. Keawkamrop, L.G. Asirvatham, A.S. Dalkilic, H.S. Ahn, O. Mahian, S. Wongwises, An experimental investigation of the air-side performance of crimped spiral fin-and-tube heat exchangers with a small tube diameter, Int. J. Heat Mass Tran. 178 (2021), 121571.
[12] X. Yu, J. Feng, Q. Feng, Q. Wang, Development of a plate-pin fin heat sink and its performance comparisons with a plate fin heat sink, Appl. Therm. Eng. 25 (2005) 173–182.
[13] F. Zhou, N. Hansen, I. Catto, Numerical prediction of thermal and hydraulic performance of heat sinks with enhanced heat transfer capability, in: Proceedings of the ASME/JSME 2011 8th Thermal Engineering Joint Conference AJTEC2011, 2011. Honolulu, Hawaii, USA.
[14] W. Yuan, J. Zhao, C.P. Tso, T. Wu, W. Liu, T. Ming, Numerical simulation of the thermal hydraulic performance of a plate pin fin heat sink, Appl. Therm. Eng. 48 (2012) 81–88.
[15] M. Khoshvaght-Aliabadi, S.M. Hassani, S.H. Mazloumi, Performance enhancement of straight and wavy miniature heat sinks using pin-fin interruptions and nanofluids, Chem. Eng. Process: Process Intensification 122 (2017) 90–108.
[16] K. Nilpueng, H.S. Ahn, D.W. Jerng, S. Wongwises, Heat transfer and flow characteristics of sinusoidal wavy plate fin heat sink with and without crosscut flow control, Int. J. Heat Mass Tran. 137 (2019) 565–572.
[17] P. Teertstra, M.M. Yovanovich, J.R. Culham, Analytical forced convection modeling of plate fin heat sink, Proceedings of the 15th IEEE Semi-Thermal Symposium (1999) 34–41.
[18] H.-H. Wu, Y.-Y. Hsiao, H.-S. Huang, P.-H. Tang, S.-L. Chen, A practical plate-fin heat sink model, Appl. Therm. Eng. 31 (2011) 984–992.